

Performance Assessment of Mechanical and Durability Properties of Cupola Slag Geopolymer Concrete with Fly and Rice Husk Ashes

Stephen Adeyemi Alabi*, Jeffrey Mahachi

Department of Civil Engineering Technology, University of Johannesburg, Doornfontein Campus, Johannesburg, South Africa



ABSTRACT: Research into substituting recycled materials for cement and aggregates can yield beneficial natural resource conservation, waste management, cost savings, and reduced embodied energy in concrete. Hence, this research investigates the potential adoption of coal fly ash (CFA) and rice husk ash (RHA) as geopolymer binders to partially substitute cement in varying proportions up to 25%. However, cupola furnace slag (CFS) was also used as a partial substitute of crushed granite from 0% to 35% in steps of 5% in the production of geopolymer concrete (GPC). The selected geopolymer binders were synthesized using an alkaline solution. Workability, compressive strength, and rapid chloride penetration tests on fresh and hardened normal concrete (NC) as control and GPC containing CFS were evaluated at different water-binder ratios. The findings revealed that integrating 15% CFA, 20% RHA, and 30% CFS with w/b of 0.50 and 0.65 improved the workability by 180% and 105.7%, respectively, but compressive strength is significantly reduced. The findings further showed that combining 75% OPC, 20% CFA, 5% RHA, 100% RS, 20% CFS, and 80% CG results in optimal compressive strength of 19.68 N/mm² and, 21.49 N/mm² at 28 days and 56 days with w/b of 0.50, respectively, as contrasted to the lowest possible strength requirement. The Rapid Migration Test (RMT) was used to determine the chloride ions permeability in various concrete mixes. The results show that GPC produced with the combination of 15% CFA, 20% RHA 65% OPC, 30% CFS, and 70% CG with w/b of 0.65 is more durable and has higher chloride ion penetration resistance than most other mix proportions.

KEYWORDS: Chloride ion; Compressive strength; Cupola furnace slag; Geopolymer concrete; Pozzolans.

[Received Jun. 21, 2021; Revised Nov. 24, 2021; Accepted Mar. 15, 2022]

Print ISSN: 0189-9546 | Online ISSN: 2437-2110

I. INTRODUCTION

Waste recycling and re-use have become necessary due to rising demand, diminishing reserves, and increased pressure on natural deposits to make concrete. The potential utilization of recycled aggregates and pozzolanic cement in place of traditional aggregates and cement can benefit natural resource conservation, waste management, and cost reduction. The utilization of recyclable materials in construction are becoming more popular as people become more aware of the vast amount of waste generated every day due to modern lifestyles, extensive resource exploitation, and environmental concerns (Lau *et al.*, 2014; Murali *et al.*, 2012).

Furthermore, cement clinker production is energy-intensive and environmentally unfriendly, with large amounts of CO₂ emitted depleting the ozone layer (Thiedeitz *et al.*, 2020). As a result, there is a need for non-traditional cementing materials that are innovative, environmentally friendly, effective, and affordable. Pozzolans are a possible replacement material. Similarly, cupola furnace slag (CFS) is a viable substitute for traditional coarse aggregate and cement. The evolution of concrete production a short time ago has resulted in new sustainable concrete types. Geopolymer concrete (GPC) is one such concrete (Pilehvar *et al.*, 2018; Yazdi *et al.*, 2018). GPC is a type of eco-friendly concrete that

eliminates or reduces the utilization of Portland cement in concrete (Abdollahnejad *et al.*, 2019; Shalika and Hemant, 2016; Torres-Carrasco *et al.*, 2015). It is the mixture of alkaline solution and pozzolans such as coal Fly ash (CFA) (Bouaissi, *et al.*, 2019; Parveen *et al.*, 2018; Nuaklong *et al.*, 2017) Silica fume (SF) (Mo *et al.*, 2016), rice husk ash (RHA) (Alabi and Mahachi, 2020), Ground Granulated Blast furnace slag (GGBS) Panesar *et al.*, 2017; Islam *et al.*, 2015), and waste glass powder (Demirel *et al.*, 2018; Tho-In *et al.*, 2017) as source materials having almost the same mechanical and physical properties as compared to ordinary Portland cement (OPC) (Lim *et al.*, 2018; Vistin *et al.*, 2017; Un *et al.*, 2015). Geopolymer has appealing properties that have prompted several researchers to look into this type of concrete (Gholampour *et al.*, 2019; Zabihi *et al.*, 2018; Mohseni, 2018; Nath and Sarker, 2015). Despite this, a small number of researchers have reported that geopolymer concrete has higher compressive strength and chloride-ion resistance (Mesgari *et al.*, 2020; Saloni *et al.*, 2020; Saini and Vattipalli, 2020; Bouaissi, *et al.*, 2019; Noushini and Castel, 2018). These studies, however, have had little or no application in buildings and infrastructures in harsh environments. However, there appears to be no study based on the combination of CFA and RHA as a geopolymer binder in the production of GPC utilizing CFS as a partial replacement of coarse aggregate. The

*Corresponding author: aalabi@uj.ac.za

innovative utilization of pozzolanic geopolymer cement (PGC) containing CFS will provide less expensive and environmentally friendly concrete.

In practice, due to differences in the quality and grade of the products, other concrete constituents, and the interactivity of the various components, most countries have variations in the production and performance of GPC using these by-products. Currently, there is little GPC activity in the South African construction industry and most developing countries such as Nigeria (Attwell, 2014). Consequently, comprehensive studies on local materials, demands, and capacities are required to understand possibilities. As a result, it is necessary to investigate local materials to optimize concrete mixtures that will significantly impact sustainability. However, this study reported the mechanical and durability of CFS-based GPC containing CFA and RHA as a combined binder. The compressive strength and chloride-ion resistance obtained from different replacements of traditional aggregates (granite) with CFS; and OPC with CFA and RHA were used to assess the best combination of CFS, CFA, and RHA. The GPC-based CFA and RHA's compressive strength was tested at 7, 28, and 56 days compared to concrete without CFS, CFA, or RHA (control). Oxide composition and microstructure analyses were performed using X-ray Fluorescence (XRF), X-ray Diffraction (XRD), and Scanning Electron Microscope to distinguish the interaction in the material formation and morphological structure of CFA and RHA (SEM).

II. MATERIALS AND METHODS

A. Materials

The materials used in this study include water, ordinary Portland cement (OPC), rice husk ash (RHA), coal fly ash (CFA), river sand (RS), alkaline activator, crushed granite (CG), and cupola furnace slag (CFS). The details of the properties of these materials and how they were obtained are described below:

1) Water

In the production of GPC, water is essential. In other words, water was used to hydrate cement, moisten aggregate, mix the concrete constituents, and cure. The portable water used in this study conformed to the recommendation of ASTM 1602 (2012).

2) Binding materials

OPC is the most common binding material used as an essential concrete ingredient worldwide. The class 42.5 of OPC conforming to BS 12 (1996) was used. The cement class number denotes its lowest possible compressive strength that the cement is presumed to achieve within 28 days. To avoid being affected by atmospheric conditions, adequate care was made to ensure that the procurement was made from a single bunch in an impermeable paper bag. The cement quality in terms of its chemical and physical properties was tested to follow ASTM C127-12 (2012) and ASTM C114-04 (2004) recommendations.

Rice husk (RH) has been certified as one of the potential pozzolanic materials majorly from agricultural waste and is available in a large quantity worldwide each year (Fapohunda *et al.*, 2021; Piyarat *et al.*, 2021; Thiedeitz *et al.*, 2020; Nalobile *et al.*, 2019; Akeke *et al.*, 2016). It is one of the

source materials used as a geopolymer binder activated with alkaline liquids in this study. The RH was procured in an Ekiti State paddy field. Then it was incinerated for more than 24 hours in an open space at a relative temperature of about 700 °C. After that, the RH was allowed to burn gradually and was allowed to cool, before collecting the ash for further testing. The ash was grounded for approximately 2 hours in a Los Angeles (LA) mill before being taken through a mesh with a size of 0.074 mm opening.

The CFA used in this study as a source material was procured from a thermal energy plant in Lokoja. CFA is a natural, organometallic outcome of coal from thermal energy plants. It is a cementitious material with no binding properties. When calcium hydroxide is chemically reacted at room temperature in the presence of moisture, a compound with cementitious properties is formed. Calcium silicate hydrates are formed when aluminosilicates in the CFA interact with calcium ions in water.

i) Alkaline activator

An 8M sodium hydroxide (NaOH) and sodium silicate (Na_2SiO_3) mixture with a mix proportion of 1:2.5 was used as an alkaline solution to synthesize the geopolymer binders. Because of the significant heat emission, the alkaline solutions were mixed a day before making geopolymer concrete.

ii) Aggregates

The river sand (RS) is used as a fine aggregate. However, this is usually blended with other concrete constituents to fill the pores with the concrete matrix. The grading pattern of the RS was carried following the recommendation of BS 812 (1985). Hence, the outcome revealed that the specimen meets the general classification limit recommended by BS 882 (1992). The measured values of some selected physical properties of RS such as bulk density, specific gravity, fineness modulus, moisture content, and absorption rate are 1.82, 2.34, 1390 kg/m³, 7%, and 2.42, respectively.

A smooth-surfaced CG obtained from a quarry site in Akure metropolis was used as coarse aggregate. The aggregate size being used for concrete production varies from 10 mm to 19 mm. The measured values of some selected physical properties of CG, such as specific gravity, fineness modulus, absorption rate, and bulk density, are 2.65, 5.78, 1.86, and 1635 kg/m³, respectively. Figure 1 shows a sieve analysis of crushed granite. It was discovered that the CG used met the ASTM D6913/D6913M-17 requirements (2017), including specifications for both wearing and non-wearing surfaces. The aggregate crushing value (ACV) standard values range between 30 and 45, according to BS 812: Part 104 (1985). The average ACV for CG was determined to be 30.4. Also, the aggregate impact value (AIV) value of the CG was around 23.1.

The CFS was collected in huge quantities from the Foundry Dump Site within Akure Metropolis. The slag was taken to the Laboratory, scrubbed, and separated to remove visible earth contaminants (Alabi and Mahachi, 2020; Afolayan and Alabi, 2013). The material was therefore crushed into fragments varying in size from 10 to 19 mm. CFS was used as a partial substitute for CG in the development of GPC. Figure 1 presents the particle distribution of CFS. The

measured values of some selected physical properties of CFS, such as specific gravity, absorption rate, and bulk density, are 2.57, 1.81, and 1810 kg/m³.

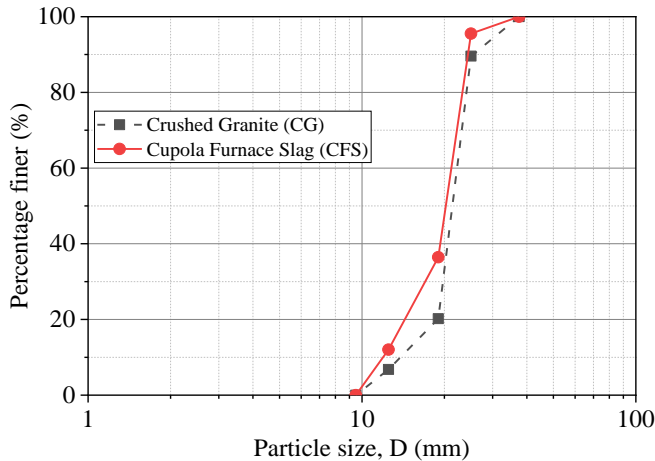


Figure 1: The grain size distribution of crushed granite (CG) and cupola furnace slag (CFS).

B. Making of GPC Specimens

1) GPC mix design

There is presently no unified guideline capable of producing GPC (Li *et al.*, 2019). Hence, this implies that the design of the GPC mix is based mainly on experimentation. As a result, in designing concrete grade C15/20, a mix ratio of 1:2:4 by weight of binder, fine and coarse aggregates were used.

2) Experimental setup for the production of GPC

In this study the potential adoption of coal fly ash (CFA) and rice husk ash (RHA) as geopolymer binders to partially substitute cement (0%, 5%, 5%, 10%, 20%, 15%, 10%, and 20% for CFA; and %, 5%, 10%, 10%, 5%, 20%, 25%, and 20% for RHA, by weight of cement) was studied. However, cupola furnace slag (CFS) was also used as a partial substitute of crushed granite from 0% to 35%, in steps of 5% in the production of geopolymer concrete (GPC). The strategy for mixing GPC samples is comparable to those used to make Portland cement concrete (PCC). All aggregates used in the production of concrete were maintained at saturated surface dry conditions (SSD). First, all the aggregates, together with CFS, were blended for approximately 5 minutes.

The CFA and RHA were therefore introduced and rigorously dry blended for about 3 to 6 minutes. The alkaline compound was introduced slowly and blended for approximately 8 minutes till a homogenous composition was noticeable. To augment the flowability of the fresh concrete blends, extra water was supplemented and thoroughly mixed. Table 1 shows atypical concrete mixes considered in this study. A slump experiment was done and recorded on the new GPC. The resulting fresh GPC was placed into three layers and compacted with a conventional rod in a standard concrete cube. After 24 hours at a temperature of 27±2°C, the specimens were taken away from the formworks, weighed, and kept underwater for 24 hours to cure at room temperature. Three specimens were taken from the water every 7 days for 56 days, at which point the weights were measured and

assessed for compressive strength. The strength measurements were taken as a mean of three specimens.

For each mix proportion, specimens 50 mm thick and 100 mm in diameter were produced to investigate the durability of GPC (see Table 1). Six samples were produced and assessed for each of the proportions at 7 days and 56 days. The samples were protected with a polyurethane sheet and moist cured at an ambient temperature of 23±2°C till the test days. The Rapid Migration Test (RMT) was used to determine chloride ions' permeability for various GPC mixtures. The samples were immersed in the solution (300 ml of 10 percent NaCl solution and 250 ml of 0.1NaOH solution) for 7 and 56 days, respectively, before being removed and tested for chloride ion penetration depth. A migration cell with a 15V applied voltage was set up. The current flowing through each cell was measured. After 6 hours, the samples were removed, split, and the chloride ions penetration depth for each specimen was determined using the colorimetric technique. A colorimetric indicator of 0.1 N Silver Nitrate was used, similar to the method used by Otsuki *et al.*, (1992) and Tang and Nilsson, (1994).

3) Characterization of pozzolanic materials

The microstructural/morphological features of the CFA and RHA were examined using a high-resolution Zeiss Sigma Field Emission Scanning Electron Microscope (FE-SEM)® equipped with both backscattered and Oxford energy dispersive X-ray (EDX) detectors. The FE-SEM was set to backscattered electron imaging (BSE) mode at 15 kV to distinguish the CFA and RHA phases. EDX spot and area analyses were used to determine the compositional variations in the CFA and RHA. The number of phases present was determined. X-ray diffraction (XRD) patterns displaying CFA and RHA samples' mineralogical characteristics were quantitatively obtained by measuring within the range of 2θ = 5° – 90° using a Bruker D2 phaser® diffractometer equipped with a cobalt K radiation source. The pattern is generated by the crystals' organized formations (materials) in the components and provides an essential understanding of the crystalline morphology of the CFA and RHA samples. The machine was run at a temperature of 25°C with a generator set to 30 kV and 10 mA. The obtained pattern was analyzed using PANalytical (v3.0e) X'pert HighScore software. X-ray fluorescence spectrometry was also used to evaluate the oxide composition of OPC, CFA, and RHA.

III. RESULTS AND DISCUSSION

A. Composition Analysis and Microstructure of Raw Materials

Table 2 and 3 presents the chemical composition results and physical properties of OPC, RHA, and CFA using XRF. The most usual identified elements present in CFA, RHA, and OPC are Ca, Fe, Mg, Na, and K. The variation may be due to harvest year, geographic factors, and paddy fields. However, the levels of the identified elements were different across the pozzolans samples analyzed. The sum of silicon dioxide (SiO₂), aluminum oxide (Al₂O₃), and ferric oxide (Fe₂O₃) of CFA is 92.38%, which is accompanied by a low calcium oxide (CaO) content of 1.72%. Furthermore, CFA is more

pozzolanic because the sum of those oxides in pozzolan should be at least 70%. RHA has a SiO₂ content of 87.83%, which is significantly higher than that of CFA. According to Table 2, the specific gravities of RHA are slightly higher than that of CFA.

The XRD patterns of CFA and RHA are shown in Figures 2 and 3. CFA mainly was in the crystalline form of SiO₂ with a single grain size orientation, as shown in Figure 2(a). The degree of structural order, on the other hand, is very high (i.e., 84.62 percent). Because of the broad peak at a 2θ angle of about 22°, the RHA is mostly amorphous, as shown in Figure 2(b).

Table 1: Experimental concrete mix design.

Concrete mix	Binding Materials			Fine Aggregate	Coarse Aggregates		Water Content	
	OPC (kg/m ³)	CFA (kg/m ³)	RHA (kg/m ³)	RS (kg/m ³)	CFS (kg/m ³)	CG (kg/m ³)	(W/B) _{0.50} (kg/m ³)	(W/B) _{0.65} (kg/m ³)
Control	174.91	0	0	349.81	0	699.63	87.46	113.69
GPC1	157.42	8.75	8.75	349.81	34.98	664.65	87.46	113.69
GPC2	148.67	8.75	17.49	349.81	69.96	629.67	87.46	113.69
GPC3	139.93	17.49	17.49	349.81	104.94	594.69	87.46	113.69
GPC4	131.18	34.98	8.75	349.81	139.93	559.70	87.46	113.69
GPC5	113.69	26.24	34.98	349.81	209.89	489.74	87.46	113.69
GPC6	113.69	17.49	43.73	349.81	174.91	524.72	87.46	113.69
GPC7	104.95	34.98	34.98	349.81	244.87	454.76	87.46	113.69

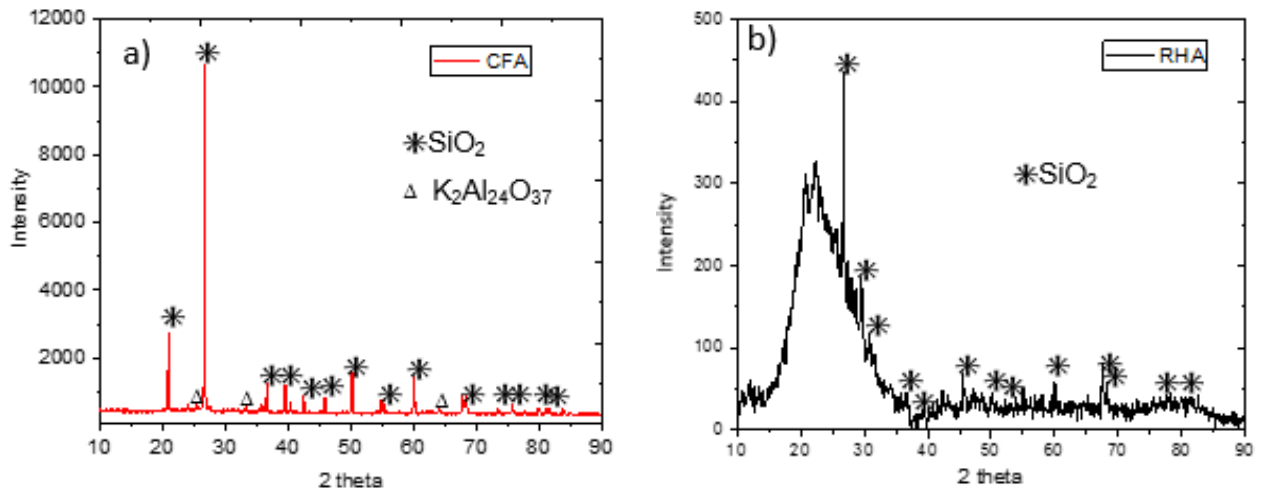


Figure 2: X-ray Diffraction (XRD) pattern of a) coal fly ash, (CFA) and b) rice husk ash, (RHA).

Table 2: Chemical and physical properties of OPC, RHA, and CFA.

Oxide composition (%)	CFA	RHA	OPC
CaO	1.72	0.68	61.52
SiO ₂	57.2	87.83	21.02
Al ₂ O ₃	28.6	0.46	5.78
Fe ₂ O ₃	6.58	0.67	3.28
MgO	1.78	0.44	2.08
Na ₂ O ₃ /K ₂ O	2.81	3.03	0.78
SO ₃	0.02	-	2.04
LOI	1.18	5.81	8.34
Specific gravity	2.21	2.34	2.95

The silicate crystallization at a 2θ angle of about 27° indicates that the RHA was burned at temperatures higher than 700°C. The RHA was discovered to be grey. The ignition loss, on the other hand, was significantly higher. This may be attributable to the ash's high concentration of unburned carbon content.

Back Scattered Detector (BSD) images of coal fly ash (CFA) and rice husk ash (RHA) can be seen in Figure 3. The lumps of about 100 μm can be seen from the figure, which may have been formed due to particle agglomeration. The pozzolans (CFA and RHA) had distinct morphological characteristics. The CFA and RHA particles studied were irregularly shaped and ridged. In other words, CFA and RHA particles have spherical and angular shapes, respectively. The observed shape of RHA particles is an essential characteristic in the concrete application as a binder. Energy Dispersive X-ray (EDX) area analysis on different spots, that is, on the light and dark regions, was used to identify the phases present in the RHA and CFA. Figures 4 and 5 show the average composition of the phases obtained from EDX for RHA and CFA, along with representative EDX spectra.

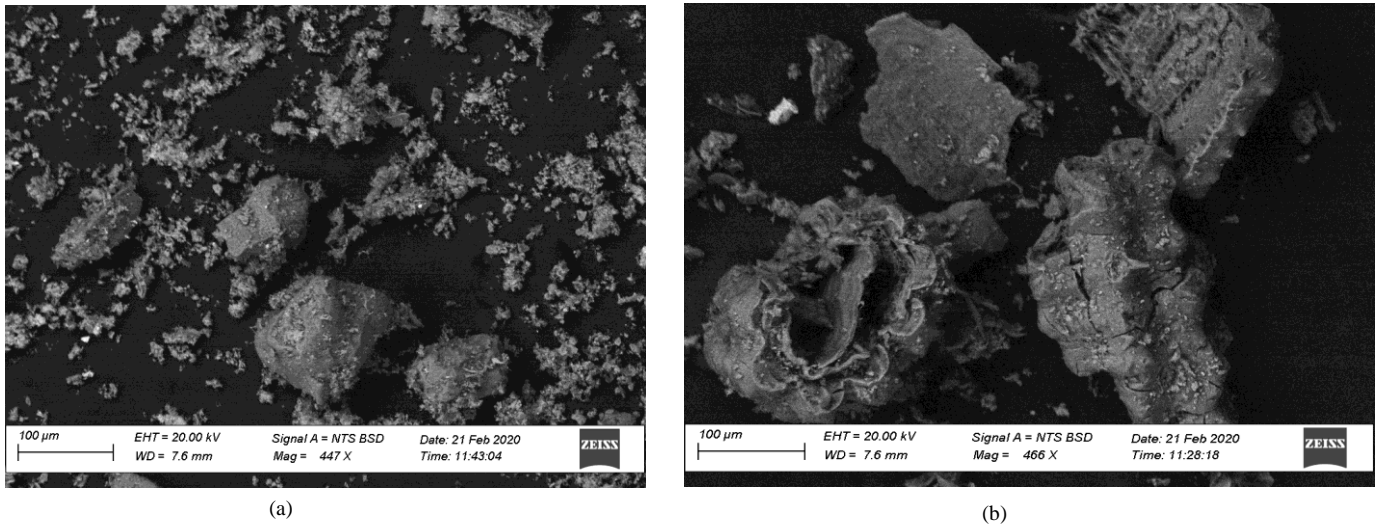
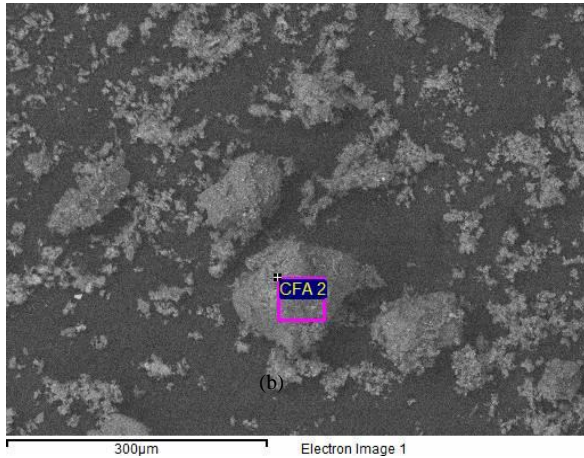


Figure 3: Back Scattered Detector (BSD) images of (a) coal fly ash, (CFA) and (b) rice husk ash, (RHA).



Element	Weight (%)	Atomic (%)
O K	57.27	70.76
Al K	2.33	1.70
Si K	37.51	26.40
K K	0.54	0.27
Ti K	0.57	0.24
Fe K	1.79	0.63
Totals	100.00	

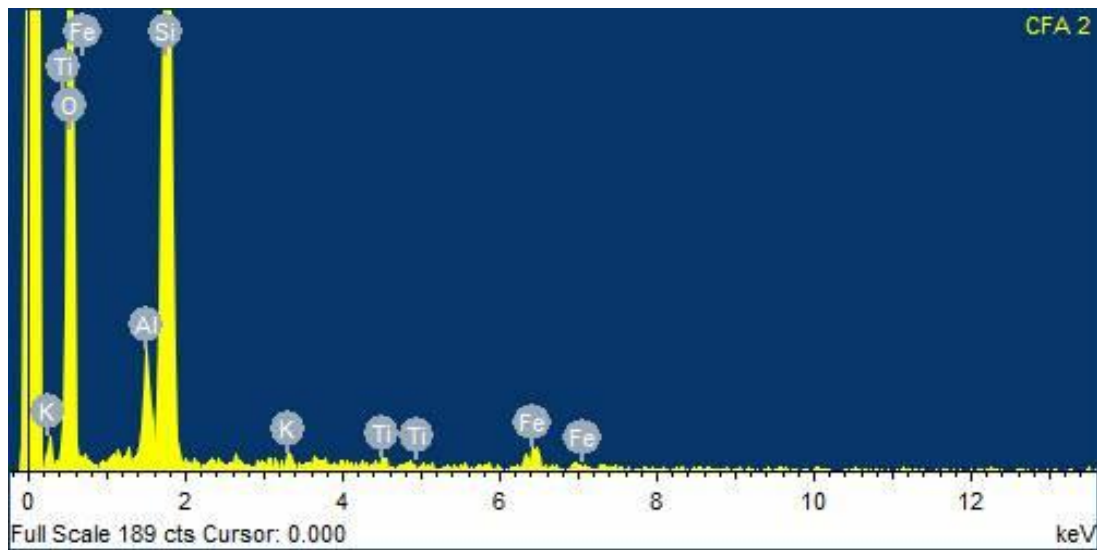
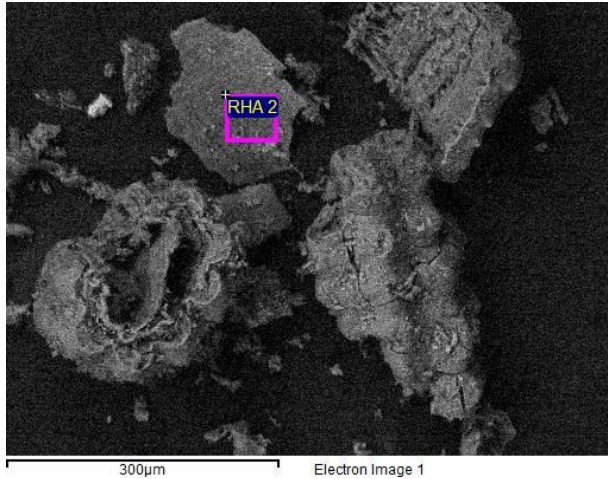
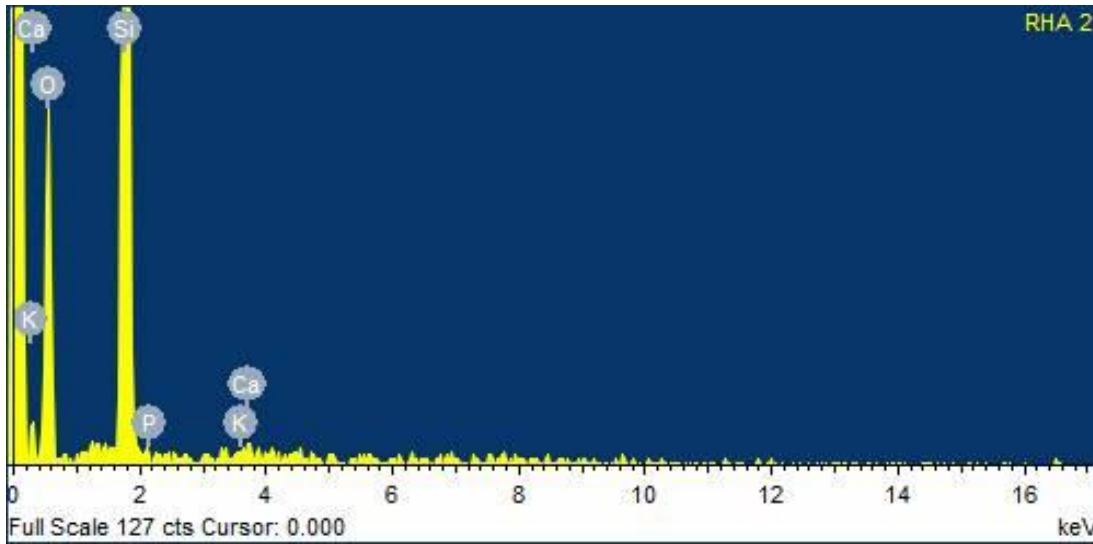


Figure 4: Energy Dispersive X-Ray (EDX) area analysis showing (a) the composition and (b) spectra of the CFA.



Element	Weight (%)	Atomic (%)
O K	52.58	66.22
Si K	45.88	32.92
P K	0.51	0.33
K K	0.73	0.38
Ca K	0.30	0.15
Totals	100.00	

(a)



(b)

Figure 5: Energy Dispersive X-Ray (EDX) area analysis showing the composition and spectra of the RHA.

A. Slump Test

Figure 6 depicts the slump test results of the fresh concrete mixes. The slump values were found to be higher in all GPC mixes containing CFS with a w/b ratio of 0.50 than in the control sample. On the other hand, slump values range between 24 mm (GPC1) and 55 mm (GPC7), while the control has 20 mm. Except for GPC7, which had medium workability. The slumps of all mixes averaged 37.7 mm, indicating low workability. As a result, such concrete may be suitable for foundations and light reinforcement rather than standard reinforced concrete work.

Using a w/b ratio of 0.65, the slump increased slightly in all mixes. The slump varied between 38 mm (GPC1) and 72 mm (GPC7), with a mean of 54 mm. This indicates that the concrete has medium workability because it falls within the

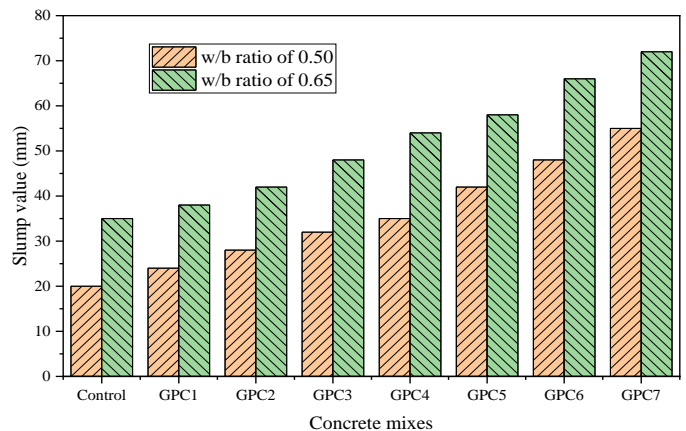


Figure 6: Slump value of different fresh concrete mixes.

standard range of 50–90 mm. This concrete is appropriate for simple strip footings and cast-in-place hard-standing slabs. On the other hand, the low workability observed could be attributed to the lower CFA and RHA contents, which may not fill the pores of the mixes and bind well with other constituents. However, because of their ability to absorb free water, concrete mixtures with higher levels of hybrid alkali-activated binders had higher slump values.

Many factors, in general, can be said to have contributed to the low workability of the GPC. The samples were mixed in the laboratory while dry, implying less water was available, as the aggregates require some water to wet their surfaces. As a result, the water content was not adjusted to account for dry aggregates. The physical properties of the aggregates, such as fineness modulus and shapes, were also discovered to influence workability. The water absorption of the fine aggregate used in this study exceeds the ASTM C127-15 maximum limit of 2.3% (2015). The greater the water absorption, the more water is required to produce workable concrete. According to Rangan (2010), the molar concentration of sodium hydroxide has a significant effect on the workability of GPCs. As a result, all slump values were within the ACI 211.1 (1991) range for various constructions.

B. Compressive Strength

Figure 7 depicts the effect of different percentage replacements of recycled aggregate (CFS) and hybrid alkali-activated binder (OPC/CFA/RHA) contents on the compressive strength of GPC with various water-binder ratios. Compressive strength generally increases with curing age. The compressive strength was found to decrease as the CFS and binders' content varied. It was also discovered that water-binder ratios have only a minor impact on strength development. In other words, GPC samples with a lower water-binder ratio ($w/b = 0.50$) have greater compressive strength than samples with a higher water-binder ratio ($w/b = 0.65$).

Moreover, since RHA and CFA contain a high Si content, the decrease in strength may be due to change in the Si/Al ratio. However, according to De Silva *et al.*, (2007) and Tho-In *et al.*, (2017), this may significantly alter the properties of GPC while causing relatively minor changes in Si and Al contents during aluminosilicate geopolymerization. Furthermore, the development of low-crosslinked aluminosilicate materials resulting from a high Si/Al ratio may be responsible for decreased compressive strength (Rattanasak *et al.*, 2010; Tho-In *et al.*, 2017).

For $w/b = 0.50$, the compressive strength of normal concrete (control) increased by 69.37%, 72.89%, and 2.08% from 7 days to 28 days, 7 days to 56 days, and 28 days to 56 days, respectively. As a result, the strength development from 28 days to 56 days was relatively slow compared to other days. Hence, this could be due to insufficient binder hydration

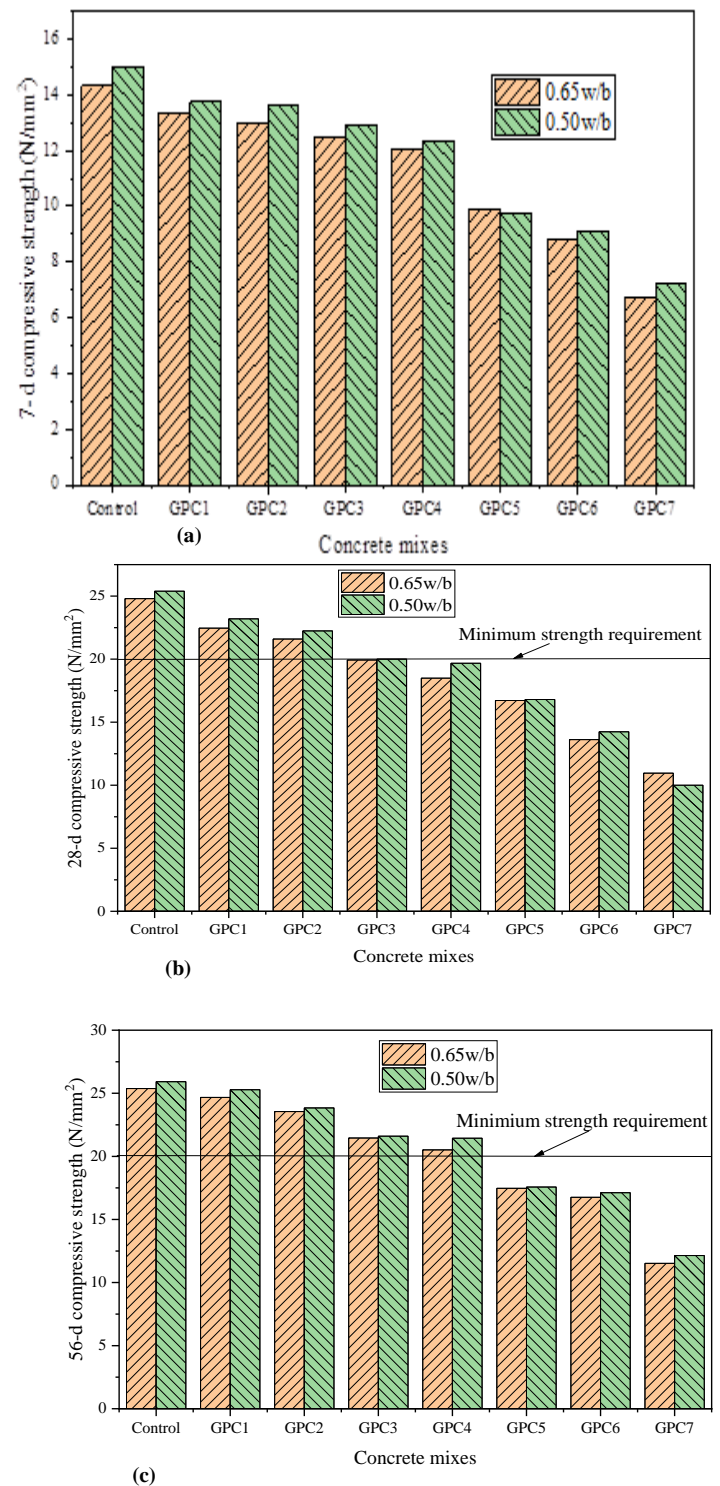


Figure 7: Compressive strength development at (a) 7 days, (b) 28 days and (c) 56 days with w/b of 0.50 and 0.65.

at the interfacial zone (ITZ). However, the control sample's strength increased by 73.18%, 77.21%, and 2.32% from 7 days to 28 days, 7 days to 56 days, and 28 days to 56 days, respectively, at $w/b = 0.65$. The control samples with a w/b of 0.65 developed greater strength than the control

samples with a w/b of 0.50. It was also discovered that as the CFS and binder contents increased, the compressive strengths at all ages gradually decreased with w/b.

Furthermore, the maximum increase in compressive strength of GPCs with w/b of 0.65 was approximately 68.14%, 66.67% percent, 59.34%, 53.52%, 68.55%, 54.45%, and 63.10% from 7 days to 28 days. In w/b of 0.50 from 7 days to 28 days, the maximum compressive strength increase observed for GPCs was approximately 68.61%, 63.34%, 54.51%, 54.74%, 72.13%, 56.14%, and 38.89%. Similarly, the maximum compressive strength increase of GPCs with w/b of 0.65 from 7 days to 56 days was approximately 84.67%, 81.73%, 71.48%, 70.25%, 76.13%, 90.02%, and 71.43%. The observed maximum increase in compressive strength for concrete mixes in w/b of 0.50 at 7 days to 56 days was approximately 83.72%, 75.09%, 66.87%, 74.03%, 80%, 87.72%, and 68.67%.

However, for both w/b considered, a relatively slow increase in the concrete mixes' compressive strength from 28 days to 56 days was also observed. Hence, this could be because most geopolymerization reactions occur during the early stages of concrete curing. Control concrete developed early strength faster than other GPC, as shown in Figure 9. The amount of CFA and hybrid binders in GPC decreases its strength. This could be attributed to the high water absorption capacity of the binders or the pozzolanic activity of the microparticles of the binders when combined with cement compounds. Finally, compressive strengths of 19.68 N/mm² and 21.49 N/mm² are obtained at 28 days and 56 days from specimens containing 20% CFS, 70% OPC, 5% RHA, and 20% CFA, with compressive strengths of 19.68 N/mm² and 21.49 N/mm², respectively. In contrast to the designed strength of 20 N/mm², the compressive strength of normal concrete (control) is 25.39 N/mm² at 28 days and 25.92 N/mm² at 56 days, with a w/b of 0.50.

The compressive strength of concrete produced with w/b ratios of 0.50 and 0.65 did not differ significantly, as shown in Figure 8. The ratio of control sample compressive strength to GPC compressive strength for both w/b ratios was also discovered to be heavily influenced by GPC compressive strength, as the ratio decreased with increasing GPC compressive strength and varies between 1.09 and 2.54 at compressive strength up to 23.2 N/mm².

C. Chloride ion Penetration Performance of GPC

Figures 9 and 10 show the relative effect of the charge passed on the GPC at 7 and 56 days with varying w.b ratios. However, some GPC had lower charges passed than the control concrete, especially concrete blends with a w/b of 0.50. Charge reductions ranged from 500 mA to 1500 mA at 7 days with a w/b of 0.50; 900 mA to 1700 mA at 56 days with a w/b of 0.50; 320 mA to 600 mA at 7 days with a w/b

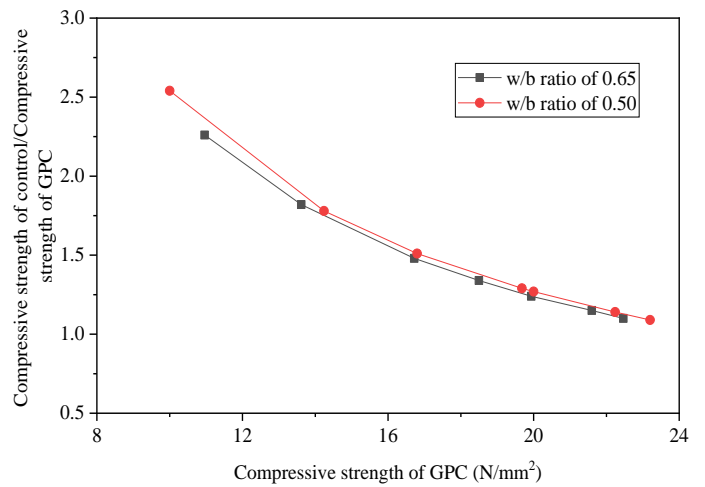


Figure 8: The ratio of compressive strength of control to the compressive strength of GPC against compressive strength of GPC. at 28 days.

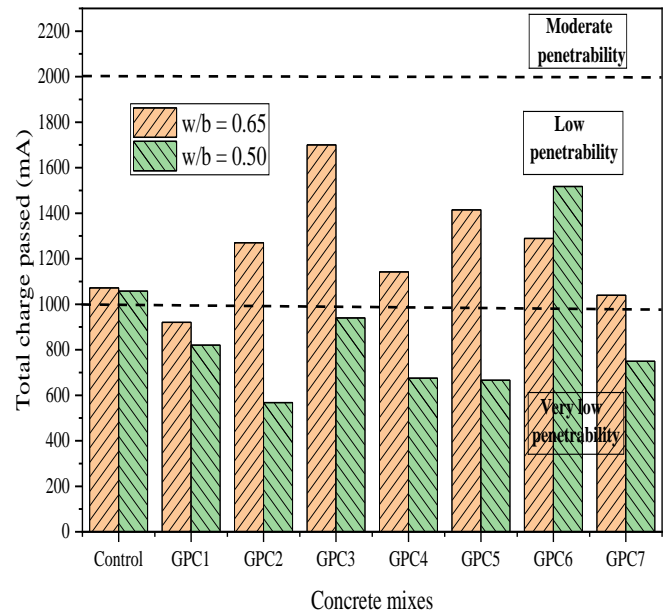


Figure 9: Total charge passed at 7-d of GPCs with different water-binder ratios.

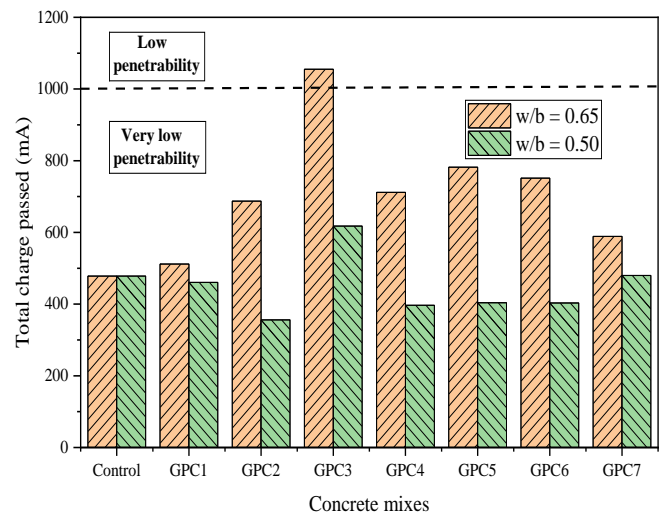


Figure 10: Total charge passed at 56-d of GPCs with different water-binder ratios.

of 0.65; and 480 mA to 1200 mA at 56 days with a w/b of 0.65. This may be mainly attributable to the micro-filler effect of the RHA and CFA, which also caused matrix densification.

On the other hand, the difference in current variability before and after chloride-ion passes through the specimen shows that the effects of other ions in the pore solution on the current are negligible. This means that chloride ion ratio to other ions in the pore solution is assumed to be constant after the chloride-ion passage. It is also evident in Figs. 9 and 10 that current variations in control samples decrease reasonably fast at 7 and 56 days compared to samples made with different binders.

Figure 11 depicts chloride ion penetration depth after 7 and 56 days of curing for control concrete samples and GPCs with a w/b ratio of 0.65. GPC5 has a final depth of 8 mm, GPC6 has a final depth of 15 mm, and GPC3 has a final depth of 19 mm. GPC7, GPC2, GPC1, and GPC4 have final depths of 20 mm, 25 mm, 30 mm, and 30 mm, respectively. With a final depth of 10 mm, it is evident that the control sample is resistant to chloride. As a result, only GPC2 outperformed the control sample after 7 days with a w/b ratio of 0.65. The addition of hybrid binders and recycled coarse aggregate improved the permeability resistance of concrete. GPC5 is far more durable after 56 days of curing, with a final depth of penetration of 7 mm, followed by GPC6 with a final depth of penetration of 11 mm, and then GPC1 and GPC7 with final penetration depths of 14 mm. GPC2, GPC3, and GPC4 have final depths of 16 mm, 16 mm, and 22 mm, respectively, while the control sample has a final depth of 8 mm. In this particular instance, GPC5 outperformed the control sample and thus lasted longer. In general, adding hybrid binders to GPCs improved their durability. Mixes with a w/b ratio of 0.50 had the same trend as mixes with a w/b ratio of 0.65, as shown in Figure 12. At 7 days, only GPC3 performed exactly like the control sample. All 56 days mixes performed poorly with a

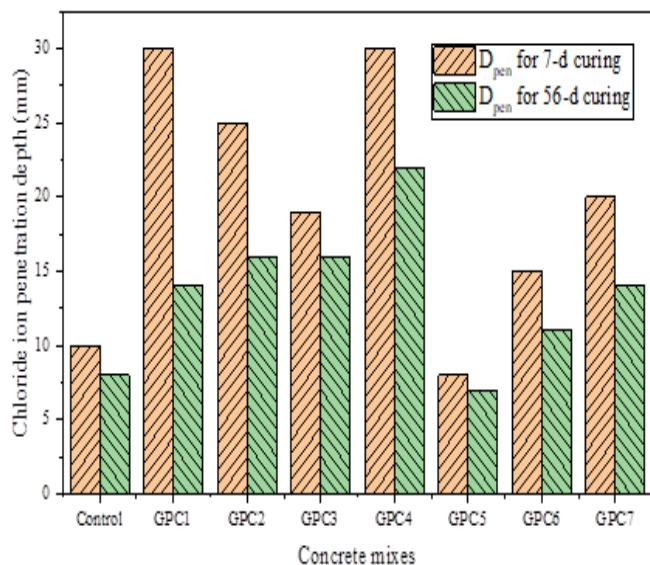


Figure 11: Chloride ion penetration depth for the control and GPCs at w/b of 0.65.

w/b ratio of 0.50. It can be concluded that the w/b ratio has a significant influence on the chloride ion penetration performance of concrete.

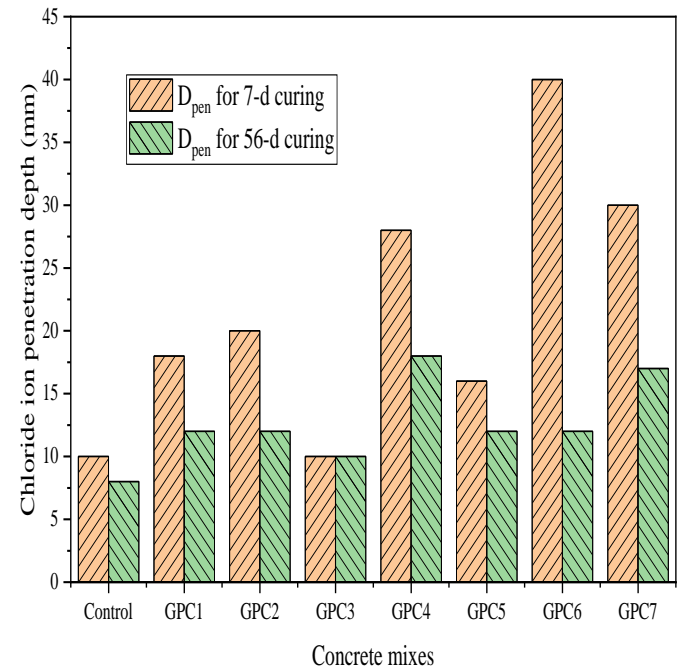


Figure 12: Chloride ion penetration depth for the control and GPCs at w/b of 0.50.

It was observed for all samples in general, that the resistance to chloride-ion penetration increased with the number of curing days. The implication is that as curing days increase, so will the durability of the concrete. Previous studies on chloride ion penetration produced comparable results for various GPC (Ikumapayi *et al*, 2019). The improved interfacial zone and the reduced average pore size of the concrete contributed to the increased chloride penetration resistance. The GPC has a relatively high resistance to chloride penetration, because of its lower median pore diameter and porosity values.

Furthermore, the hydrated structures of control samples contain more $\text{Ca}(\text{OH})_2$. The reaction of the binders with the obtainable $\text{Ca}(\text{OH})_2$ from OPC allows for complete binder hydration, resulting in higher quality concrete structure with the least potential porosity. These findings and those of many other researchers highlight the benefits of incorporating pozzolans into concrete exposed to aggressive conditions to reduce chloride ion penetration (Ikumapayi *et al*, 2019). It is worth noting that, regardless of w/b, chloride ion penetration depth increased as the binders and CFS contents increased in most mixes.

Chloride penetration depth was found to reduce with increase in the concrete age (see Figures 11 and 12) which implies that the age of the concrete can improve its resistance to chloride migration. It was also discovered that concrete with a w/b ratio of 0.50 has significantly better chloride

penetration resistance regardless of age than mixes with a w/b ratio of 0.65. The high alumina (Al_2O_3) content of CFA can cause a pozzolanic reaction with cement to produce tricalcium aluminate ($3\text{CaO}\cdot\text{Al}_2\text{O}_3$ or C_4A), which may be responsible for the chemical binding of chloride ion in GPCs to form Friedel's salt ($\text{Ca}_6\text{Al}_2\text{O}_3\cdot\text{CaCl}_3\cdot 10\text{H}_2\text{O}$).

IV. CONCLUSION

The mechanical and durability performance of cupola furnace slag geopolymer concrete-based CFA and RHA is reported in this paper. A comprehensive set of laboratory experiments was conducted to estimate the workability, compressive strength, and rapid chloride penetration of fresh and hardened concrete at water-binder ratios of 0.50 and 0.65. The concrete mix with the lowest compressive strength has the highest slump value, according to the GPC experiment results. It has been observed that the compressive strength of concrete decreases as CFA and binder content increases. As the curing ages increased, so did the control and GPC. It has been observed that the water-binder ratio has a direct relationship with compressive strength.

Based on the chloride ion penetration test results for GPCs performed using RMT, it is possible to conclude that the GPC has higher chloride ion penetration resistance than the samples made from different mixes. As a result, GPC has become more durable, particularly in harsh or coastal environments. The partial replacement of OPC and CG in concrete production, particularly with 15% CFA, 20% RHA, 65% OPC, 30% CFS, and 70% CG, improves its durability. In general, resistance to chloride-ion penetration increased with the number of curing days and as a result, the concrete durability may change with age. Eventually, the geopolymers used have a natural, environmentally friendly sustainability. It can contribute positively to the significant decrease of global greenhouse gases and the overall sustainability of building materials.

ACKNOWLEDGMENT

The authors wish to acknowledge the support of the University Research Committee (URC) and the Faculty Research Committee (FRC) of the University of Johannesburg, South Africa.

REFERENCES

- Abdollahnejad Z.; M. Mastali, M. Falah, T. Luukkonen, M. Mazari and M. Illikainen. (2019).** Construction and Demolition Waste as Recycled Aggregates in Alkali-activated Concretes. *Materials*, 12(23): 1-22.
- ACI 211.1 (1991).** Standard Practice for Selecting Proportions for Normal, Heavyweight, and Mass Concrete. Published by American Concrete Institute.
- Afolayan, J. O. and Alabi, S. A. (2013).** Investigation on the Potentials of Cupola Furnace Slag in Concrete. *International Journal Integrated Engineering*, 5(2): 59-62.
- Akeke, G. A.; D. E. Ewa, and F. O. Okafor, (2016).** Effects of Variability in the Pozzolanic Properties of Rice Husk Ash on the Compressive Strength of Concrete. *Nigerian Journal of Technology*, 35(4): 694-698.
- Alabi, S. A. and Mahachi J. (2020).** Assessment of the Ternary Coarse Aggregates for Economic Production of Sustainable and Low-Cost Concrete. *Journal of Materials and Engineering Structures*, 7(1): 25-34.
- Alabi, S. A. and Mahachi, J. (2020).** Behavior of Ground Cupola Furnace Slag Blended Concrete at Elevated Temperature. *Journal of Materials and Engineering Structure*, 7(1): 35-46.
- ASTM 1602, (2012).** Standard Specification for Mixing Water Used in the Production of Hydraulic Cement Concrete, ASTM International, West Conshohocken, PA.
- ASTM C114-04, (2004).** Standard Test Methods for Chemical Analysis of Hydraulic Cement. ASTM International, West Conshohocken, PA.
- ASTM C127-12, (2012).** Standard Test Method for Density, Relative Density (Specific Gravity), and Absorption of Coarse Aggregates, Annual Book of ASTM Standards, ASTM International, West Conshohocken, PA.
- ASTM C127-15 (2015).** Standard Test Method for Relative Density (Specific Gravity) and Absorption of Coarse Aggregate, ASTM International, West Conshohocken, PA.
- ASTM D6913/D6913M-17, (2017).** Standard Test Methods for Particle-Size Distribution (Gradation) of Soils Using Sieve Analysis, ASTM International, West Conshohocken, PA.
- Attwell, C. (2014).** Geopolymer Concrete: A Practical Approach. Paper Presented at International Conference of Construction 678 Materials and Structures, Johannesburg 466-466.
- Bouaissi, A.; L. Y. Li, M. M. A. Abdullah and Q. B. Bui. (2019).** Mechanical Properties and Microstructure Analysis of FA-GGBS-HMNS Based Geopolymer Concrete. *Construction and Building Materials*, 210: 198-209.
- BS 12, (1996).** Specification for Portland Cement. British Standard Institution, London, United Kingdom.
- BS 812: Part (104) (1985).** Testing Aggregates, Part 104: Methods for Determination of Particle Size Distribution – Section 103.1 Sieve Tests, Published under the authority of the Board of BSI, The Direction of the Cement, Gypsum, Aggregates and Quarry Products Standards Committee, London.
- BS 882, (1992).** Aggregate from Natural Sources for Concrete, Published under the authority of the Board of BSI, the direction of the Cement, Gypsum, Aggregates and Quarry Products Standards Committee, London.
- De Silva, P.; K. Sagoe-Crenstil and V. Sorovivatnanon. (2007).** Kinetics of Geopolymerization: Role of Al_2O_3 and SiO_2 . *Cement and concrete Research*, 37(4): 512-518.
- Demirel, S.; H. O. Oz, M. Günes, F. Çiner and S. Adm. (2018).** Life-Cycle Assessment (LCA) Aspects and Strength Characteristics of Self-Compacting Mortars (SCMs) incorporating Fly Ash and Waste Glass PET. *The International Journal of Life Cycle Assessment*, 24(6): 1139-1153.
- Fapohunda, C.; A. Kilani, B. Adigo, L. Ajayi, B. Famodimu, O. Oladipupo and A. Jeje. (2021).** A Review of Some Agricultural Wastes in Nigeria for Sustainability in the Production of Structural Concrete, *Nigerian Journal of Technological Development*, 18(2): 76-87.

- Gholampour, A.; V. Dac Ho and T. Ozbakkaloglu. (2019).** Ambient-Cured Geopolymer Mortars Prepared with Waste-Based Sands: Mechanical and Durability-Related Properties and Microstructure. *Composites Part B: Engineering*, 160: 519-534.
- Ikumapayi, C. M.; C. Arum and P. G. Oguntunde. (2019).** Chloride Ion Penetration Performance of Biogenic Pozzolanic Cement Concrete. *ABUAD Journal of Engineering Research and Development*, 2(2): 68-77.
- Islam, A.; J. U. Alengaram, Z. M. Jumaat, A. S. M. Kabir and I. I. Bashar. (2015).** Engineering Properties and Carbon Footprint of Ground Granulated Blast-Furnace Slag-Palm Oil Fuel Ash-based Structural Geopolymer Concrete. *Construction and Building Materials*, 101(1): 503–521.
- Lau, T. L.; W. Elleithy, W. K. Choong, T. Y. Tze, C. M. Lee and A. L. Modhwadia. (2014).** Effects of Recycled Aggregates on Concrete Strengths. *Materials Research Innovations*, 18(6): 372-374.
- Li, N.; C. Shi, Z. Zhang, H. Wang and Y. Liu. (2019).** A Review on Mixture Design Methods for Geopolymer Concrete. *Composites Part B: Engineering*, 178: 107490
- Lim, J. H.; B. Panda and Q. C. Pham. (2018).** Improving Flexural Characteristics of 3D Printed Geopolymer Composites with In-Process Steel Cable Reinforcement. *Construction and Building Materials*, 178: 32–41.
- Mesgari, S.; A. Akbarnezhad and J. Z. Xiao. (2020).** Recycled Geopolymer Aggregates as Coarse Aggregates for Portland Cement Concrete and Geopolymer Concrete: Effects on Mechanical Properties. *Construction and Building Materials*, 236(1): 117571.
- Mo, H. K.; J. U. Alengaram and Z. M. Jumaat. (2016).** Structural Performance of Reinforced Geopolymer Concrete Members: A Review. *Construction and Building Materials*, 120: 251–264.
- Mohseni, E. (2018).** Assessment of Na_2SiO_3 to NaOH Ratio Impact on the Performance of Polypropylene Fiber-Reinforced Geopolymer Composites. *Construction and Building Materials*, 186: 904–911.
- Murali, G.; C. M. V. Vardhan, G. Rajan, G. J. Janani, N. S. Jajan, and R. Ramya-Sri. (2012).** Experimental Study on Recycled Aggregate Concrete. *International Journal of Engineering Research and Applications (IJERA)*, 2: 407-410.
- Nalobile, P.; J. M. Wachira, J. K. Thiong'o and J. M. Marangu. (2019).** Pyroprocessing and the Optimum Mix Ratio of Rice Husks, Broken Bricks and Spent Bleaching Earth to Make Pozzolanic Cement. *Heliyon*, 5(9): e02443.
- Nath, P. and Sarker, P. K. (2015).** Use of OPC to Improve Setting and Early Strength Properties of Low Calcium Fly Ash Geopolymer Concrete Cured at Room Temperature. *Cement and Concrete Composites*, 55, 205-214.
- Noushini, A. and Castel, A. (2018).** Performance-based Criteria to Assess the Suitability of Geopolymer Concrete in Marine Environments using Modified ASTM C1202 and ASTM C1556 methods. *Materials and Structures*, 51: 146.
- Nuaklong, P.; V. Sata and P. Chindaprasirt. (2017).** Properties of Metakaolin-High Calcium Fly Ash Geopolymer Concrete Containing Recycled Aggregate from Crushed Concrete Specimens. *Construction and Building Materials*, 161, 365–373.
- Otsuki, N.; S. Nagataki and K. Nakashita. (1992).** Evaluation of AgNO_3 Solution Spray Method for Measurement of Chloride Penetration into Hardened Cementitious Matrix Materials. *ACI Materials Journal*, 89: 587-592 .
- Panesar, D. K.; K. E. Seto and C. J. Churchill. (2017).** Impact of the Selection of Functional Unit on the Life Cycle Assessment of Green Concrete. *International Journal of Life Cycle Assessment*, 22: 1969-1986.
- Parveen, D. Singhal, M. T. Junaid, B. B. Jindal and A. Mehta. (2018).** Mechanical and Microstructural Properties of Fly Ash based Geopolymer Concrete incorporating Alccofine at Ambient Curing. *Construction and Building Materials*, 180: 298–307.
- Piyarat, N.; U. Wangrakdiskul and P. Maingam. (2021).** Investigations of the Influence of Various Industrial Waste Materials Containing Rice Husk Ash, Waste Glass, and Sediment Soil for Eco-Friendly Production of Non-Fired Tiles. *AIMS Materials Science*, 8(3): 469–485.
- Rangan, B. (2010).** Fly Ash based Geopolymer Concrete. *Proceedings of the International Workshop on Geopolymer Cement and Concrete*. Mumbai, India, Allied Publishers Private Limited, 68-106.
- Rattanasak, U.; P. Chindaprasirt and P. Suwanvitaya. (2010).** Development of High Volume Rice Husk Ash Alumino Silicate Composites. *International Journal of Minerals, Metallurgy and Materials*, 17: 654-659.
- Saini, G. and Vattipalli, U. (2020).** Assessing Properties of Alkali Activated GGBS based Self-Compacting Geopolymer Concrete using Nano-Silica. *Case Studies in Construction Materials*, 12 e00352.
- Saloni, Parveen and T. W. Pham. (2020).** Enhanced Properties of High-Silica Rice Husk Ash-based Geopolymer Paste by Incorporating Basalt Fibers. *Construction and Building Materials*, 245 118422
- Shalika, S. and Hemant, S. (2016).** Abrasion Resistance of Geopolymer Concrete at Varying Temperature. *Journal of Mechanical and Civil Engineering*, 13(1), 22-25.
- Tang, L. and Nilsson, L. O. (1992).** Chloride Diffusivity in High Strength Concrete. *Nordic Concrete. Research*, 11: 162-170.
- Thiedeitz, M.; W. Schmidt, M. Härder and T. Kränkel, (2020).** Performance of Rice Husk Ash as Supplementary Cementitious Material after Production in the Field and in the Lab. *Materials*, 13: 4319.
- Tho-In, T.; V. Sata, K. Boonserm and P. Chindaprasirt. (2018).** Compressive Strength and Microstructure Analysis of Geopolymer Paste using Waste Glass Powder and Fly Ash. *Journal of Cleaner Production*, 172: 2892-2898.
- Torres-Carrasco, M. and Puertas, F. (2015).** Waste Glass in the Geopolymer Preparation, Mechanical and microstructural characterization. *Journal of Cleaner Production*, 90: 397-408.
- Un, C. H.; G. J. Sanjayan, S. R. Nicolas, V. J. S. J. Deventer. (2015).** Predictions of Long Term Deflection of

Geopolymer Concrete Beams. *Construction and Building Materials*, 94: 10–19.

Vistin, P.; M. M. S. Ali, M. Albitar and W. Lucas. (2017). Shear Behaviour of Geopolymer Concrete Beams Without Stirrups. *Construction and Building Materials*, 148: 10–21.

Yazdi, M. A.; M. Liebscher, S. Hempel, J. Yang, and V. Mechtcherine. (2018). Correlation of Microstructural and

Mechanical Properties of Geopolymers Produced from Fly Ash and Slag at Room Temperature. *Construction and Building Materials*, 191: 330-341.

Zabihi, S. M.; H. Tavakoli and E. Mohseni. (2018). Engineering and Microstructural Properties of Fiber-Reinforced Rice Husk–Ash based Geopolymer Concrete. *Journal of Materials in Civil Engineering*, 30(8): 04018183.